In: EUSAR 2022: 14th European Conference on Synthetic Aperture Radar, Leipzig, 25-27 July 2022
https://ieeexplore.ieee.org/document/9944217

Through-Wall Multistatic Polarimetric 3D SAR

Daniel Andre[a], Richard Sabiers[a], Mark Finnis[b]
[a] Centre for Electronic Warfare Information and Cyber, Cranfield University, Defence Academy of the United Kingdom
[b] Centre for Defence Engineering, Cranfield University, Defence Academy of the United Kingdom

Abstract

Through-Wall (TW) Synthetic Aperture Radar (SAR) imagery can be difficult to interpret due to several factors including signal attenuation in highly cluttered environments, target overlay, difficult to interpret low SAR resolution and low frequency scattering responses. One approach which may help improve image interpretability is to employ 2D SAR apertures with multiple distributed receivers in all polarizations. For example: a 2D SAR aperture would allow the formation of 3D images, reducing noise levels and clutter overlay, as well as improving the recognition of objects through providing height information; the distributed receivers would be more likely to capture any bright specular responses from targets in the scene, making them visible; the polarimetric collection may provide useful target information, such as its orientation, polarizability or number of interactions with the radar signal. Highlight results from TW-SAR bistatic polarimetric experiments at the Cranfield University GBSAR laboratory are presented, illustrating the utility of the approach.

1. Introduction

Through-Wall (TW) Synthetic Aperture Radar (SAR) images can be difficult to interpret due to factors including signal attenuation, highly cluttered environments, target overlay due to the 3D nature of the scene, low SAR resolution and low frequency scattering responses which can be resonant in nature.

An approach which can help improve image interpretability is to employ 2D SAR apertures with multiple distributed receivers in all polarizations. For example, the 2D SAR aperture would allow the formation of 3D SAR images which would reduce noise levels and clutter overlay, as well as improving the recognition of objects through providing height information. If the receivers are distributed about the scene, the multistatic aperture would be more likely to capture any bright specular responses from targets in the scene, making them more visible. A polarimetric collection could provide further useful target information, such as its orientation, polarizability or number of interactions with the radar signal.

This paper presents selected results from TW-SAR bistatic polarimetric experiments performed recently at the Cranfield University GBSAR laboratory, illustrating the utility of the approach. Section 2 describes the bistatic polarimetric decomposition employed in the study; Section 3 discusses the laboratory measurements, describing the laboratory system, some results on canonical scatterers and on a mock building structure with targets inside.

2. Bistatic polarimetric decomposition

Whilst monostatic polarimetric decompositions are well understood, bistatic generalizations of these are not well-known and the physical interpretation of many proposed are not clear. Some bistatic decomposition approaches are only slight modifications of existing monostatic approaches, for example simply introducing an anti-symmetric component to the target scattering matrix (which is always symmetric in the monostatic case). However the physical meaning associated with this polarimetric parameter extraction may be unclear, and increasingly so where the geometry is far from the monostatic case.

The approach selected for application in this work, is that described by Titin-Schnaider [1-3], constituting a bistatic generalization of the Huynen Fork parameter decomposition [4], providing six polarimetric parameters: for the bistatic case there are two Orientation angles and two Symmetry angles associated with the “entry” and “scattered” ray directions. The formalism has been related to a generalization of the Cloude-Pottier parameters [3].

The bistatic generalization of the Huynen Fork target parameters was found to provide a physically meaningful pixel based polarimetric decomposition [2]. In the monostatic case there are four parameters of interest θ τ ν γ (theta, tau, nu, gamma) representing:

- **Orientation / Tilt angle**, θ: linked to the angle between the projection of the scatterer main axis and the horizontal reference angle: $-90° \leq \theta \leq 90°$. Here we define a positive rotation as clockwise about the down-range direction. Scatterers for which the tilt angle may be meaningful include rods / dipoles and straight edges of extended objects.
- **Symmetry angle**, τ: allowing the separation of symmetric and non-symmetric scatterers. A symmetric scatterer is symmetric about a plane containing the incident ray, $0° \leq |\tau| \leq 45°$, where 0° indicates high symmetry, and $|\tau| = 45°$ indicates low symmetry. Scatterers with high symmetric would include spheres, rods / dipoles and corner reflectors.
- **Skip angle**, ν: divides scatters into two classes according, approximately, to whether the scattered rays have had an odd or even number of bounces: $0° \leq |\nu| \leq 45°$, where 0° indicates an Odd bounce interaction and $|\nu| = 45°$ indicates an Even

bounce interaction. Odd bounce scatterers include spheres, flat plates and trihedral multi-bounce. Even bounce scatterers include dihedral multi-bounce. Note that at certain aspects the dihedral response may be dominated by single flat plate responses or straight edge diffraction.

- **Polarizability angle**, γ: in this approach is taken to mean that the scatterer only returns waves with a particular polarization regardless of incident polarization, hence a polarization projection: $0° \leq \gamma \leq 45°$, where 0° indicates high polarizability and 45° low. Scatterers with medium to high polarizability include rods and the straight edges of extended objects. Scatterers with low polarizability include spheres, flat plates, corner reflectors with multi-bounce including both dihedrals and trihedrals.

For the bistatic case there are two τ parameters, τe τs, and two θ parameters, θe θs, – "e" stands for the entry / incident direction, and "s" stands for the scattered direction. In the monostatic case these directions are equivalent, so that the τ values become the same, and the θ values become the same. It is noted that once the orientation parameters are determined (θe, θs), the additional Huynen parameters provide information intrinsic to the electromagnetic mechanism itself, that is, independent of input and output antenna orientations.

3. Laboratory measurements

3.1 SAR measurement System

The radar measurements were performed with a vector network analyser, and over the frequency band 1-4 GHz in a space approximately 8m by 8m in the horizontal and 4m in the vertical, seen in Figure 3-1 top. Initially single polarization wideband microwave horns were used, so that to achieve the four linear polarization combinations these had to be successively rotated for the different scans. In latter experiments dual polarization horns were used, controlled via microwave switches. The horns are seen in a monostatic configuration in Figure 3-1 top, where they are mounted on a scanning system which can move them across an aperture 3.5 m wide and 1.5 m tall, providing a 2D SAR aperture. For the bistatic SAR collections, the receiver horn was placed on a tripod at specific locations about the scene, leaving the transmitter on the scanner (Figure 3-1 bottom). Combinations of spheres and rods were employed for system calibration [5].

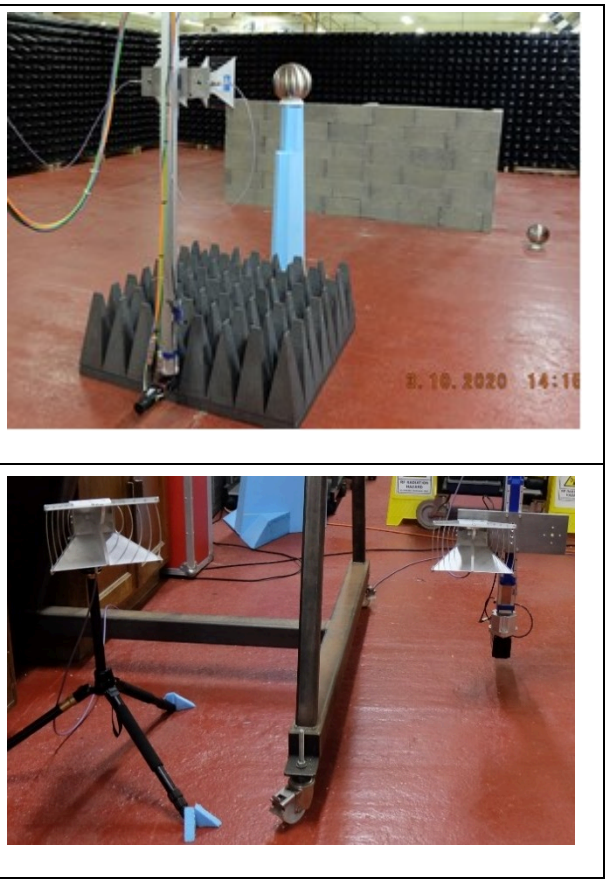

Figure 3 1, Microwave antennas in monostatic configuration undergoing calibration (top), and in bistatic configuration (bottom).

3.2 Canonical Scatterer Measurements

To test the polarimetric parameter extraction methodology, canonical reflectors were measured including spheres, corner reflectors, cylinders, rods and flat plates. In particular, the dihedral and sphere seen in Figure 3-2 were measured. The dihedral was rotated in steps of 45° from 0° to 157.5°, effectively spanning all orientations, due to the symmetry of the dihedral.

Sets of quad-polarised SAR images were generated for each dihedral orientation, which allowed per-pixel polarimetric parameter extractions, allowing the generation of colourized polarimetric SAR image results.

Dihedral SAR images for the 90° orientation is presented in Figure 3-3. The colourized SAR image in Figure 3-3 left shows the Skip (ν) parameter extraction, where red is associated with $|\nu|=0°$ or Odd-bounce, and green is associated with $|\nu|=45°$ or Even-bounce. Radar down-range corresponds to the direction up the page. It is noted that the brightness of the images is given by the polarimetric Span $|VV|^2 + |VH|^2 + |HH|^2 + |HV|^2$, but the colour is given by the extracted parameter angle with association shown in the figure colour bar.

Figure 3-2, Sphere and dihedral targets. The dihedral was rotated to multiple angles.

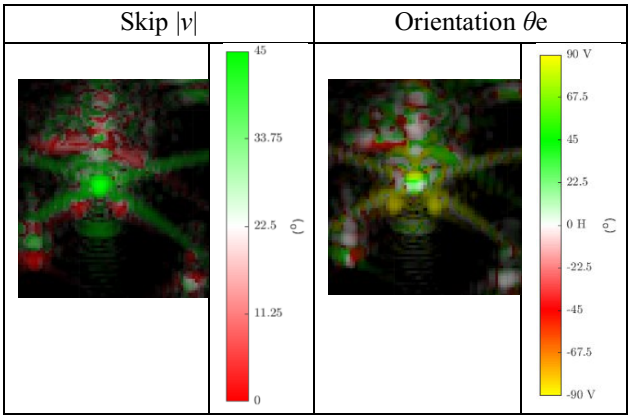

Figure 3-3, Colourized SAR images with Huynen Skip parameter |ν| (left), and Huynen Orientation parameter θe (right). Targets visible include the raised sphere (bottom-left) and dihedral (centre), showing the signature response for the 90° dihedral orientation. The two leading edges of the dihedral "De" are visible.

The triplet of signatures seen on the bottom-left of the image correspond to the raised sphere, where: the closest range signature is the direct sphere interaction and is seen to be Odd-bounce, the next is thought to have a single multipath interaction with the ground and is seen to be Even-bounce, and the third is thought to have had two multipath interactions with the ground and is seen to be Odd-bounce again.

The bright central signature is the main dihedral response. It is seen to be Even-bounce as expected. The dihedral has a vertical axis orientation, so the signature is narrow in cross-range.

It is of interest to note the behaviour of the two signatures just up-range from the main dihedral signature (just below the main dihedral signature). These are the leading edge dihedral plate signatures (De). In the vertical orientation image, the leading edge signatures are two narrow red dots. Indeed, for all the dihedral orientations the "De" signatures were seen to be strongly Odd-bounce.

In Figure 3-3 right, the polarimetric SAR image showing the Orientation parameter θe is presented. The Orientation values for the sphere are recognized as being meaningless, and for the main bright signature of the dihedral they are also unclear. However for the dihedral plate leading edges "De" they are meaningful, so that in the image they show up as yellow, indicating a vertical orientation, which matches the actual dihedral orientation.

For a quantitative analysis, the polarimetric parameters of the brightest Span intensity pixel in a given signature are given in Table 3-1.

Table 3-1. Dihedral Edge (De) Huynen parameter (in °) responses for the different dihedral orientations.

Dihedral angle	θe	θs	|ν|	|τe|	|τs|	γ
0°	-1.2	0.4	22.8	1.6	1.2	30.0
22.5°	19.6	19.4	0.1	1.5	0.4	32.4
45°	44.5	43.7	1.6	0.2	0.8	30.3
67.5°	64.8	64.5	0.3	0.5	1.3	28.3
90° (= -90°)	-88.1	-87.8	0.9	1.2	0.7	23.8
112.5° (= -67.5°)	-66.0	-66.2	1.4	1.0	1.4	20.6
135° (= -45°)	-44.6	-44.5	7.9	0.2	0.9	18.2
157.5° (= -22.5°)	-22.8	-22.6	1.3	0.6	0.9	13.7

It can be seen that the extracted values for Orientation, θe and θs, closely match the actual orientations of the dihedral, although one needs to take into account that due to the symmetry of the dihedral, its actual orientation angle values have the following symmetry θ = θ±180°. Generally the De signatures were seen to have low Skip angle |ν|, being Odd bounce, have high symmetry |τe| |τs|, and the polarizabilities γ are seen to have mid-range values.

3.3 Model Building Scene

During the course of the measurement campaign, a simple mock building was constructed, seen in Figure 3-4, approximately 3m by 3m in size, with a wall height such there was no radar line of sight into the structure. Some simple targets were placed inside, including a sphere, two dihedrals and metal cabinets non-aligned with the concrete walls.

Figure 3-4, Mock concrete building with targets inside. The metal cabinets to the rear are non-aligned with structure, giving rise to specular flashes and wall-multipath visible in different bistatic geometries.

Both monostatic and bistatic 2D SAR scans were repeated for a number of geometries. In the bistatic scans, the receiver locations are fixed. In this paper, only two example polarimetric 3D SAR images are presented. Figure 3-5 shows 3D SAR image renderings of the scene, colourized by the skip angle. The monostatic image is seen in Figure

3-5 top, and an example bistatic image in Figure 3-5 bottom. The bistatic geometry has the fixed receiver positioned to the right of the 2D transmitter SAR aperture.

In the SAR images, the radar down-range direction, is aligned with the green y-axis, so that the front wall is towards the bottom of the page. Both the front wall, and the various scatterers can be seen even though they are imaged through the wall.

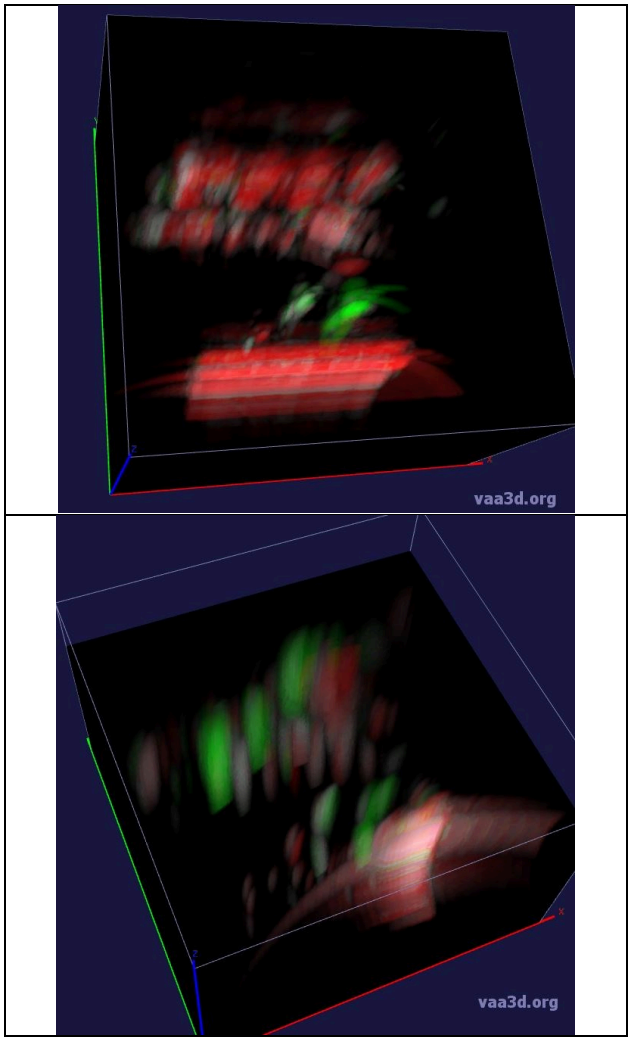

Figure 3-5, 3D polarimetric SAR images of the mock building scene. Radar down-range is aligned up the page with the green y-axis. The image is colourized according to Odd (red) and Even (green) bounce scattering, parametrized by the modulus of the Skip parameter. The top image is monostatic, whereas the bottom image is bistatic, with a fixed receiver to the right of the scene.

In the monostatic image (Figure 3-5 top), the front wall is bright and Odd-bounce (red), and the two dihedrals appear as bright Even-bounce scatterers (green). The sphere is to the left of the dihedrals, and appears as Odd-bounce. However the sphere-floor multipath signature which appears below it has a dominant Even-bounce component. From the cabinets, some Odd-bounce signatures have arisen mostly from the vertical edges, as they are not aligned with the SAR aperture. The parts of the rear wall which are not shadowed by the cabinet are visible.

In the bistatic image (Figure 3-5 bottom), only the right-hand part of the front wall is visible, as this is aligned with the mid-point of the transmit and receive antenna positions. The dihedrals and sphere signatures are visible, and again some evidence of direct scattering from the non-aligned cabinets is visible. In this bistatic geometry, three large Even-bounce signatures are evident at the rear of the scene. These correspond to multipath interactions between the cabinets and the rear wall. It is noted that with bistatic geometries where the receiver was instead to the left of the transmit receiver, the front faces of the non-aligned cabinets gave bright Odd-bounce responses.

4. Conclusion

Selected results from a through-wall monostatic and bistatic polarimetric SAR investigation were presented, from the GBSAR laboratory at Cranfield University. The system allows 2D bistatic SAR apertures to be collected in quad-polarization over wide frequency bands, of the 8m by 8m space.

Target scenes consisting of canonical scatterers allowed the evaluation of a bistatic generalisation of the Huynen polarimetric parameter extraction algorithm.

A through-wall scenario was also investigated, with monostatic and bistatic 3D SAR images generated.

Polarimetric parameters were obtained for the targets behind the wall. The scattering effects were found to be dependent upon the bistatic geometry, with target-wall multipath signatures appearing as Even-bounce, and direct signatures from other bistatic geometries as Odd-bounce.

5. References

[1] Titin-Schnaider, C. “Polarimetric Characterization of Bistatic Coherent Mechanisms”, IEEE Transactions on Geoscience and Remote Sensing, Vol.46, No.5, May 2008

[2] Titin-Schnaider, C., “Physical Meaning of Bistatic Polarimetric Parameters”, IEEE Transactions on Geoscience and Remote Sensing, Vol.48, No.5, May 2010

[3] Titin-Schnaider, C., “Characterization and Recognition of Bistatic Polarimetric Mechanisms”, IEEE Transactions on Geoscience and Remote Sensing, Vol.51, No.3, March 2013

[4] Huynen, J. R., “Phenomenological Theory of Radar Targets”, PhD Thesis, TU Delft, 1970

[5] Sarabandi, K., Ulaby, F., Tassoudji, M., “Calibration of Polarimetric Radar Systems with Good Polarization Isolation”, IEEE Transactions on Geoscience and Remote Sensing, Vol.28, No.1, January 1990

[6] Peng, H., Ruan, Z., Long, F., Simpson, J. H., and Myers, E. W. (2010) "V3D enables real-time 3D visualization and quantitative analysis of large-scale biological image data sets," Nature Biotechnology, Vol. 28, No. 4, pp.348-353. (http://vaa3d.org)

Through-wall multistatic polarimetric 3D SAR

Andre, Daniel

2022-11-10

Andre D, Sabiers R, Finnis M. (2022) Through-wall multistatic polarimetric 3D SAR. In: EUSAR 2022: 14th European Conference on Synthetic Aperture Radar, 25-27 July 2022, Leipzig, Germany
https://ieeexplore.ieee.org/document/9944217